Superconductivity competitive with checkerboard-type charge ordering in the organic conductor β-(*meso*-DMBEDT-TTF)$_2$PF$_6$

Naoki Morinaka,[1,2] Kazuyuki Takahashi,[1] Ryoma Chiba,[1,2] Fumiko Yoshikane,[1] Shoichi Niizeki,[1] Masayuki Tanaka,[3] Kyuya Yakushi,[3] Masahito Koeda,[1] Masato Hedo,[1] Tetsuya Fujiwara,[1] Yoshiya Uwatoko,[1] Yutaka Nishio,[2] Kohji Kajita,[2] and Hatsumi Mori[1,*]

[1]*Institute for Solid State Physics, The University of Tokyo, Kashiwa 277-8581, Japan*

[2]*Department of Physics, Toho University, Funabashi 274-8510, Japan*

[3]*Institute for Molecular Science, Okazaki 444-8585, Japan*

(Received 1 January 2009; revised manuscript received 27 August 2009; published 28 September 2009)

The pressure dependence of resistivity for the checkerboard-type charge-ordered (CO) molecular conductor β-(*meso*-DMBEDT-TTF)$_2$PF$_6$ has been investigated. Under the low pressure of 0.6 kbar, the temperature of resistivity minimum (T_{min}) falls from 90 K at an ambient pressure to 67 K, and after the resistivity has been increased, the superconducting (SC) transition is observed at 4.6 K. By applying magnetic field, the SC state is suppressed and the large positive magnetoresistance (MR) is demonstrated below T_{min} in the CO state. Since the positive MR was observed even in the metallic state under high pressures, the summarized pressure-temperature ($P-T$) phase diagram reveals that the SC state neighbors to the CO-insulating and charge-fluctuated metallic states.

DOI: 10.1103/PhysRevB.80.092508 PACS number(s): 74.70.Kn

I. INTRODUCTION

Since the discovery of the first organic superconductor in 1980, over 120 kinds of organic superconductors have been found.[1] These organic superconductors are categorized as either strongly correlated systems or weakly correlated systems. In the latter system, the superconducting (SC) state is competitive with the electronic states induced by the nesting of the Fermi surface, charge density wave (CDW), spin density wave (SDW), or anion ordering. The SC critical temperature (T_c) of this system is relatively low up to 2 K for TMTSF$_2$CF$_3$SO$_3$ (TMTSF =tetramethyltetraselenafulvalene),[2] although the mechanism of superconductivity for TMTSF salts is intriguing.[3] On the other hand, the T_c of strongly correlated systems is the highest among organic superconductors up to 14 K for β'-(BEDT-TTF)$_2$ICl$_2$ [BEDT-TTF =bis(ethylenedithio)tetrathiafulvalene].[4] Especially, the SC state competitive with the antiferromagnetic Mott insulating state has been extensively studied in κ-type and β'-type BEDT-TTF salts.[5] However, another strongly correlated system, where the SC state is competitive with the charge-ordered (CO) state, has been only studied theoretically;[6,7] the d_{xy} (Ref. 7) and triplet[8–10] superconductivities mediated by charge fluctuation have been theoretically proposed. These peculiarities in superconductivity have not been clarified experimentally yet, since there are few molecular conductors, whose SC states neighbor or are close to CO states. As for β''-(DODHT)$_2$PF$_6$, the summarized phase diagram demonstrates that the SC state is close to the CO state.[11] The superconductivity in the CO conductor of α-(BEDT-TTF)$_2$I$_3$ has been observed under uniaxial pressure[12] and understood theoretically mediated by spin fluctuation.[13]

Recently, we have found the pressure-induced superconductor with Tc=4.3 K under 4 kbar for β-(*meso*-DMBEDT-TTF)$_2$PF$_6$.[1,14] At an ambient pressure, the salt shows the metal-insulator transition at 90 K, originating from checkerboard-type charge ordering.[15] If the CO pattern is caused only by the intersite Coulomb interaction (V), this salt should have a border-type rather than checkerboard-type pattern. This checkerboard-type CO state is peculiar, and the application of an electric-field has not only induced the giant nonlinear conduction, but also afforded the electric-field-induced metastable state.[16]

To investigate the relationship between the checkerboard-type charge ordering and superconductivity, the temperature dependences of electrical resistivity under both pressure and a magnetic field have been measured for β-(*meso*-DMBEDT-TTF)$_2$PF$_6$. The SC phase was observed in a broad range from 0.6 kbar with Tc=4.6 K to 5.2 kbar with 2.6 K and neighbors the checkerboard-type CO-insulating state and charge-fluctuated metallic state.

II. EXPERIMENTAL

Single crystals of β-(*meso*-DMBEDT-TTF)$_2$PF$_6$ were prepared by an electrochemical method with 0.25 μA in chlorobenzene for 4–6 days. Electrical resistivity was measured by the four-probe method with a carbon paste as contacts in the range of 2–300 K and 0–9 T. The current of 10 μA is passed along the crystal long c axis and the magnetic field is also applied to c axis. The pressure is applied by utilizing a BeCu-NiCrAl cramp cell with Daphne 7373 as a pressure medium. The sample and Pb resistivies are measured simultaneously to detect the sample resistivity and the applied pressure. As shown in Fig. 1(b), the T_c of Pb pressure monitor at an ambient pressure is 7.1906 K which is the same as the reference data.[17] The average ΔT_c ($=T_{onset}-T_{offset}$) of Pb under pressures is very small, 0.0133 K, which corresponds to 0.35 kbar. This indicates the homogenious pressure is applied not only to Pb but also the sample.

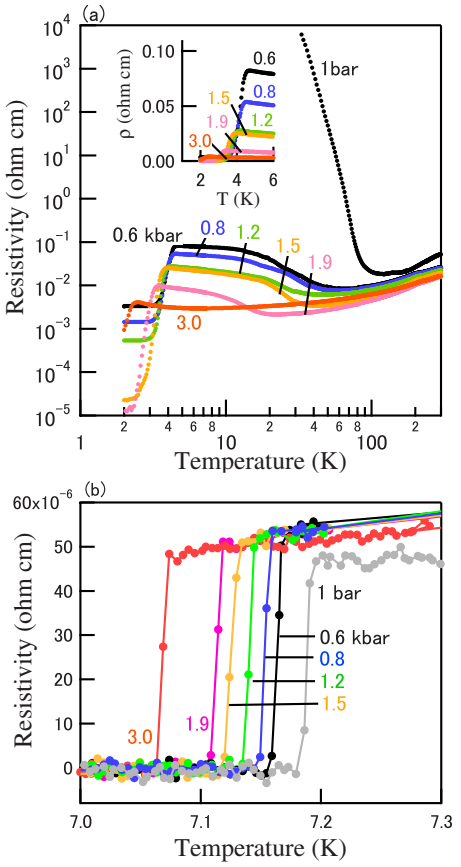

FIG. 1. (Color online) Temperature dependence of resistivity under pressure for (a) β-(*meso*-DMBEDT-TTF)$_2$PF$_6$ and (b) Pb pressure monitor.

III. RESULTS AND DISCUSSION

A. Superconducting transition under pressure

The temperature dependence of electrical resistivity at an ambient pressure for β-(*meso*-DMBEDT-TTF)$_2$PF$_6$ is illustrated in Fig. 2. The resistivity at 300 K is 0.05 Ω cm, decreases slightly down to the resistivity minimum temperature ($T_{\min}$) of 90 K, and increases sharply with a deviation at 70 K. At that temperature, the superlattice $(h,k/2,l/2)$ starts growing and becomes saturated below 50 K. The crystal

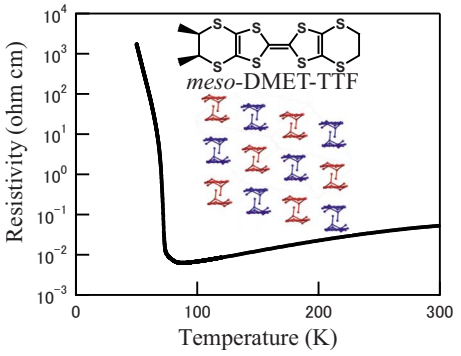

FIG. 2. (Color online) Molecular structure of *meso*-DMBEDT-TTF, long-range checkerboard-type charge-ordered state below 70 K, and temperature dependence of resistivity for β-(*meso*-DMBEDT-TTF)$_2$PF$_6$ at ambient pressure.

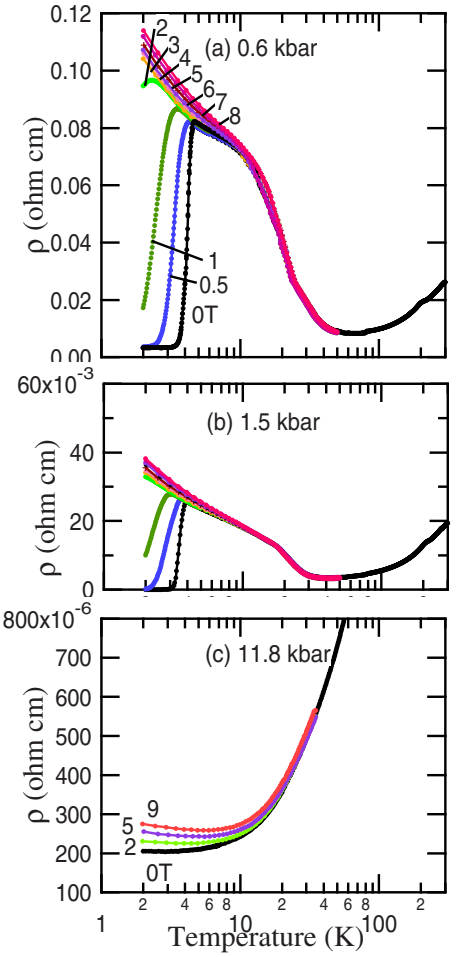

FIG. 3. (Color online) Temperature dependence of magnetoresistivity under (a) 0.6 kbar, (b) 1.5 kbar, and (c) 11.8 kbar for β-(*meso*-DMBEDT-TTF)$_2$PF$_6$.

structure analysis at 11.5 K by the synchrotron x-ray radiation reveals the checkerboard-type CO (Fig. 2); two rich charge molecules of $+0.75\times2$ and two poor charge ones of $+0.25\times2$ are arranged alternately along both the stacking and side-by-side directions.[1,15,18]

When 0.6 kbar pressure is applied to this sample, the $T_{\min}$ falls from 90 to 67 K, the resistivity increases slightly below $T_{\min}$, and the resistivity drops sharply at 4.6 K as shown in Fig. 1. This transition is confirmed to be superconductivity by the suppression of the resistivity drop when the magnetic field is applied, as shown in Fig. 3(a). This sample is very sensitive to the pressure; the CO-insulating state is suppressed rapidly and the superconductivity appears from the low pressure of 0.6 kbar, even though the $T_{\min}$ is relatively high (90 K) at an ambient pressure. The T_c also decreases when more pressure is applied, as shown in Fig. 1. All eight samples show the superconductivity with the similar pressure dependences, and the SC region is widely extended from T_c=4.6 K at 0.6 kbar to 2.6 K at 5.2 kbar with an average $dT_c/dP=-0.4$ K/kbar, smaller than in the case of BEDT-TTF salts.[17]

B. Magnetoresistance under pressure

The temperature dependences of resistivities under 0–9 T at various pressures are shown in Fig. 3. Below $T_{\min}$

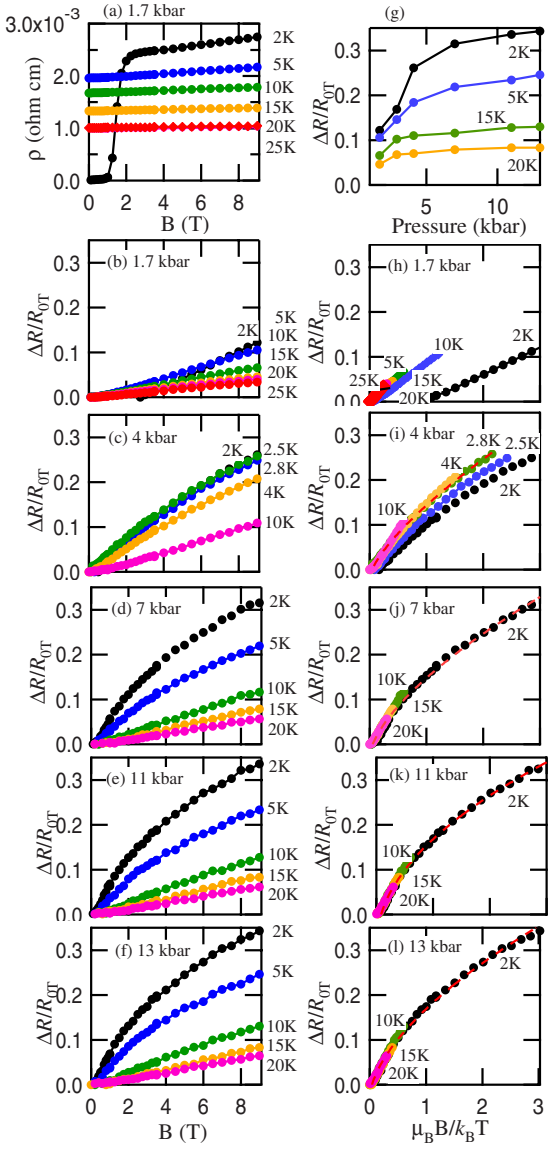

FIG. 4. (Color online) Plots of (a) resistivity, magnetoresistance as a function of magnetic field under (b) 1.7, (c) 4, (d) 7, (e) 11, (f) 13 kbar, and (g) pressure dependence of MR, MR as functions of $\mu_B B/k_B T$ under (h) 1.7, (i) 4, (j) 7, (k) 11, and (l) 13 kbar for β-(*meso*-DMBEDT-TTF)$_2$PF$_6$. The dotted lines denote the fitting of $\Delta R/R_{0T} \propto (\mu_B B/k_B T)^{\alpha}$ [α=(i)0.7, (j) 0.5, (k) 0.5, and (l) 0.6].

=67 K under 0.6 kbar and 43 K under 1.5 kbar, the resistivities increases and the large positive magnetoresistances (MR) are observed. Recently, Tanaka *et al.* reported the raman spectroscopy under pressure to identify the charge of the donor molecule (D) for β-(*meso*-DMBEDT-TTF)$_2$PF$_6$. The ν_{13} raman mode indicates $D^{0.5+}$ at 60 K under 0.8 kbar, the coexistence of $D^{0.5+}$ with the larger spectrum intensity and the CO state ($D^{0.75+}$ and $D^{0.25+}$) with the lower intensity at 58 and 55 K under 0.7 kbar, another coexistence of the CO state with the higher intensity and $D^{0.5+}$ with lower intensity at 53 K under 0.7 kbar, and only the CO state at 50 K, 40 K under 0.7 kbar and 8 K under 0.5 kbar.[16] As the charge ordering appears, the resistivity increases and MR becomes large. This agreement between transport and raman measurements was also observed under 1.5 kbar; below 40 K, the resistivity increases, MR becomes large [Fig. 3(b)], and the raman spectra indicate the appearance of charge ordering.[16] These facts show that large MR is a good indicator of the presence of the CO state.

The magnetic-field dependence of electrical resistivity under 1.7 kbar is shown in Fig. 4(a). At 2 K, the magnetic field suppresses the SC state; even in the normal state above 2.2 T the MR increases, and its ratio, $\Delta R/R_{2.2T}=(R-R_{2.2T})/R_{2.2T}$, reaches to 0.12 at 9 T. At other temperatures from 5–25 K, the ratio of MR, $\Delta R/R_{0T}$ increases up to 0.11 at 9 T [Fig. 4(b)]. When pressure is applied, $\Delta R/R_{0T}$ increases from 0.26 under 4 kbar, 0.32 under 7 kbar, and 0.34 under 11 kbar to 0.35 under 13 kbar at 2 K [Figs. 4(c)–4(f)]. Moreover, $\Delta R/R_{0T}$ is scaled with $\mu_B B/k_B T$ from 10–25 K between 1.7 and 13 kbar, where μ_B is the Bohr magneton and k_B is the Boltzmann constant [Figs. 4(h)–4(l)]. Under 1.7 and 4 kbar, this scaling is applicable above 4 K except in the SC region. Under 7, 11, and 13 kbar, MR is large even in the metallic region and scaled by $\Delta R/R_{0T} \propto (\mu_B B/k_B T)^{0.5-0.7}$ [Figs. 4(i)–4(l)], whose power law constant, 0.5–0.7, is smaller than that of conventional MR, 2. In the scaled temperature range, the similar CO electronic state is realized. The plot of $\Delta R/R_{0T}$ as a function of pressure is shown in Fig. 4(g). It is remarkable that $\Delta R/R_{0T}$ increases as the pressure is applied; this suggests that the metallic region are also in the charge-fluctuated state.

A large MR is also reported for the CO molecular conductors, θ-(BEDT-TTF)$_2$MZn(SCN)$_4$ [M=Cs,Rb], and is

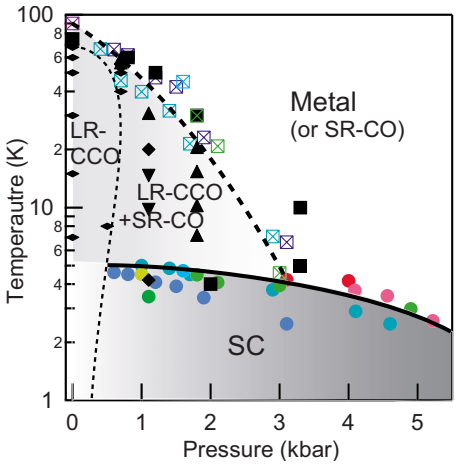

FIG. 5. (Color online) Pressure-temperature (P-T) phase diagram of electronic states for β-(*meso*-DMBEDT-TTF)$_2$PF$_6$. The solid circles and crossed squares denote the onset of SC transition temperatures (T_c) and resistivity minimum temperatures (T_{min}), respectively. The solid squares and solid thin diamonds denote the raman ν_{13} mode of metallic $D^{0.5+}$ and CO ($D^{0.75+}$, $D^{0.25+}$) states [D=*meso*-DMBEDT-TTF], respectively. Other symbols denote the coexistence of $D^{0.5+}$ and ($D^{0.75+}$+$D^{0.25+}$) spectra, where solid triangles, solid diamonds, and inverted solid triangles denote that the intensity of the $D^{0.5+}$ spectrum is higher, comparable, and lower than that of the ($D^{0.75+}$+$D^{0.25+}$) spectrum, respectively (Ref. 18). The boundaries between long-range checkerboard-type charge-ordered (LR-CCO), LR-CCO and short-range charge-ordered (SR-CO), metallic (or SR-CO), and superconducting (SC) states are shown by dotted and solid lines, respectively.

explained as a *Pauli spin blockade*; according to the Pauli exclusion principle, the localized magnetic-field-induced spins around the CO domains block conducting electrons.[20] The large MR of β-(*meso*-DMBEDT-TTF)$_2$PF$_6$ might have the same origin as the *Pauli spin blockade*. The Lorentz effect should be negligible since the current and magnetic field are applied along the same crystal long *c* axis.

The pressure—temperature (*P*-*T*) phase diagram is demonstrated in Fig. 5; at ambient pressure, the resistivity minimum temperature is 90 K ($T_{\min}$ denoted by square cross), below which the diffuse superlattice indicates the coexistence of long-range checkerboard-type charge-ordered (LR-CCO) and short-range charge-ordered (SR-CO) states, and below 70 K, the LR-CCO state is stabilized by the measurements of x-ray superlattice[15] and raman spectroscopy denoted by thin solid diamond.[18] With applying the low pressure such as 0.6 kbar, $T_{\min}$ is lowered to 67 K, and after the increase of resistivity due to the LR-CCO state, the SC state appears at 4.6 K as shown in Figs. 1 and 3(a). The onsets of all SC transition temperatures for eight samples are denoted by solid circles. The T_c decreases gradually when pressure is applied to 2.6 K under 5.2 kbar. At 1–3 kbar, the $T_{\min}$'s of resistivity measurements denoted by crossed squares agree well with the dotted boundary from the LR-CCO and SR-CO states to the metallic (or SR-CO) state, as observed by the raman spectroscopy under pressure. The solid triangles, diamonds, and inverted triangles denote that the intensity of the $D^{0.5+}$ spectrum is higher, comparable, and lower, respectively, than that of the CO ($D^{0.75+}$, $D^{0.25+}$) spectrum.[18] At more than 3 kbar above T_c, the metallic state extends, where the large MR under pressure as shown in Figs. 3(c) and 4(f) indicates that even the metallic state is in a charge-fluctuated state, namely the SR-CO state. Therefore, these measurements of electrical resistivities under various pressures and magnetic fields experimentally proves that the SC state is next to LR-CCO and SR-CO states.[19]

IV. CONCLUSION

In conclusion, the pressure dependence of resistivity at various magnetic fields for the checkerboard-type charge-ordered molecular conductor β-(*meso*-DMBEDT-TTF)$_2$PF$_6$ reveals that the SC state widely extends from T_c=4.6 K under the low pressure of 0.6 kbar to 2.6 K under 5.2 kbar, and that the SC state neighbors the LR-CCO insulating state and the SR-CO metallic state by the observation of resistivity increase and the large MR under pressure. These findings agree well with the raman spectra and are the important experimental observation that the localized and fluctuated CO states are next to the SC state.

ACKNOWLEDGMENTS

We thank H. Fukuyama, S. Mazumdar, T. Yamaguchi, and K. Yoshimi for fruitful discussions. This work was supported by Grants-in Aid for Scientific Research from MEXT (Grants No. 17540315, No. 20340087, and No. 20110007).

*hmori@issp.u-tokyo.ac.jp

[1] H. Mori, J. Phys. Soc. Jpn. **75**, 051003 (2006); H. Mori, *Introduction to Organic Electronic and Optoelectronic Materials and Devices* (CRC Press, Boca Raton, FL, 2008).
[2] R. C. Lacoe, S. A. Wolf, P. M. Chaikin, F. Wudl, and E. Aharon-Shalom, Phys. Rev. B **27**, 1947 (1983).
[3] L. Degiorgi and D. Jerome, J. Phys. Soc. Jpn. **75**, 051004 (2006); I. J. Lee, S. E. Brown, and M. J. Naughton, *ibid.* **75**, 051011 (2006).
[4] H. Taniguchi, M. Miyashita, K. Uchiyama, K. Satoh, N. Mori, H. Okamoto, K. Miyagawa, K. Kanoda, M. Hedo, and Y. Uwatoko, J. Phys. Soc. Jpn. **72**, 468 (2003).
[5] K. Kanoda, J. Phys. Soc. Jpn. **75**, 051007 (2006).
[6] H. Seo, C. Hotta, and H. Fukuyama, Chem. Rev. **104**, 5005 (2004); H. Seo, J. Merino, H. Yoshioka, and M. Ogata, J. Phys. Soc. Jpn. **75**, 051009 (2006).
[7] J. Merino and R. H. McKenzie, Phys. Rev. Lett. **87**, 237002 (2001).
[8] H. Watanabe and M. Ogata, J. Phys. Soc. Jpn. **75**, 063702 (2006).
[9] K. Yoshimi, M. Nakamura, and H. Mori, J. Phys. Soc. Jpn. **76**, 024706 (2007).
[10] M. Nakamura, K. Yoshimi, and H. Mori, J. Magn. Magn. Mater. **310**, 1099 (2007).
[11] H. Nishikawa, T. Morimoto, T. Kodama, I. Ikemoto, K. Kikuchi, J. Yamada, H. Yoshino, and K. Murata, J. Am. Chem. Soc. **124**, 730 (2002); H. Nishikawa, Y. Sato, K. Kikuchi, T. Kodama, I. Ikemoto, J. Yamada, H. Oshio, R. Kondo, and S. Kagoshima, Phys. Rev. B **72**, 052510 (2005).
[12] N. Tajima, A. Ebina-Tajima, M. Tamura, Y. Nishio, and K. Kajita, J. Phys. Soc. Jpn. **71**, 1832 (2002).
[13] A. Kobayashi, S. Katayama, K. Noguchi, and Y. Suzumura, J. Phys. Soc. Jpn. **73**, 3135 (2004).
[14] S. Kimura, T. Maejima, H. Suzuki, R. Chiba, H. Mori, T. Kawamoto, T. Mori, H. Moriyama, Y. Nishio, and K. Kajita, Chem. Commun. (Cambridge) **2004**, 2454.
[15] S. Kimura, H. Suzuki, T. Maejima, H. Mori, J. Yamaura, T. Kakiuchi, H. Sawa, and H. Moriyama, J. Am. Chem. Soc. **128**, 1456 (2006).
[16] S. Niizeki, F. Yoshikane, K. Kohno, K. Takahashi, H. Mori, Y. Bando, T. Kawamoto, and T. Mori, J. Phys. Soc. Jpn. **77**, 073710 (2008).
[17] A. Eiling and J. S. Schilling, J. Phys. F: Met. Phys. **11**, 623 (1981).
[18] M. Tanaka, K. Yamamoto, M. Uruichi, T. Yamamoto, K. Yakushi, S. Kimura, and H. Mori, J. Phys. Soc. Jpn. **77**, 024714 (2008).
[19] K. Oshima, T. Mori, H. Inokuchi, H. Urayama, H. Yamochi, and G. Saito, Synth. Met. **27**, A165 (1988).
[20] Y. Takahide, T. Konoike, K. Enomoto, M. Nishimura, T. Terashima, S. Uji, and H. M. Yamamoto, Phys. Rev. Lett. **98**, 116602 (2007).